

DISCLAIMER

This document was prepared as an account of work sponsored by the United States Government. While this document is believed to contain correct information, neither the United States Government nor any agency thereof, nor The Regents of the University of California, nor any of their employees, makes any warranty, express or implied, or assumes any legal responsibility for the accuracy, completeness, or usefulness of any information, apparatus, product, or process disclosed, or represents that its use would not infringe privately owned rights. Reference herein to any specific commercial product, process, or service by its trade name, trademark, manufacturer, or otherwise, does not necessarily constitute or imply its endorsement, recommendation, or favoring by the United States Government or any agency thereof, or The Regents of the University of California. The views and opinions of authors expressed herein do not necessarily state or reflect those of the United States Government or any agency thereof or The Regents of the University of California.

Photocatalytic generation of hydrogen from water using a cobalt pentapyridine complex in combination with molecular and semiconductor nanowire photosensitizers

Yujie Sun,^{a,c} Jianwei Sun,^{a,d} Jeffrey R. Long,^{a,d,e,*} Peidong Yang^{a,e,*} and Christopher J. Chang^{a,b,c,*}

5 Recently, a family of cobalt pentapyridine complexes of the type [(R-PY5Me₂)Co(H₂O)](CF₃SO₃)₂ (R = CF₃, H, or NMe₂; PY5Me₂ = 2,6-bis(1,1-di(pyridin-2-yl)ethyl)pyridine) were shown to catalyze the electrochemical generation of hydrogen from neutral aqueous solutions using a mercury electrode. We now report that the CF₃ derivative of this series, [(CF₃PY5Me₂)Co(H₂O)](CF₃SO₃)₂ (**1**), can also operate in neutral water as an electrocatalyst for hydrogen generation under soluble, diffusion-limited conditions on a glassy carbon electrode, as well as a photocatalyst for
10 hydrogen production using either molecular or semiconductor nanowire photosensitizers. Owing to its relatively low overpotential compared to other members of the PY5 family, complex **1** exhibits multiple redox features on glassy carbon, including a one-proton, one-electron coupled oxidative wave. Further, rotating disk electrode voltammetry measurements reveal the efficacy of **1** as a competent hydrogen evolution catalyst under soluble, diffusion-limited conditions. In addition, we establish that **1** can also generate hydrogen from neutral water under photocatalytic
15 conditions with visible light irradiation ($\lambda_{\text{irr}} \geq 455$ nm), using [Ru(bpy)₃]²⁺ as a molecular inorganic chromophore and ascorbic acid as a sacrificial donor. Dynamic light scattering measurements show no evidence for nanoparticle formation for the duration of the photolytic hydrogen evolution experiments. Finally, we demonstrate that **1** is also able to enhance the hydrogen photolysis yield of GaP nanowires in water, showing that this catalyst is compatible with solid-state photosensitizers. Taken together, these data establish that the well-defined cobalt pentapyridine complex
20 [(CF₃PY5Me₂)Co(H₂O)]²⁺ is a versatile catalyst for hydrogen production from pure aqueous solutions using either solar or electrical input, providing a starting point for integrating molecular systems into sustainable energy generation devices.

Introduction

The combination of rising global energy demands, diminishing
25 fossil fuel stores, and climate change has prompted intense interest in developing alternative carbon-neutral energy technologies. Harnessing solar energy to synthesize sustainable chemical fuels is a promising solution to the emerging energy challenge.¹⁻⁵ An appealing approach to this ultimate goal is to
30 drive chemical water splitting to hydrogen and oxygen using solar energy input,⁶ since the generation and combustion of hydrogen from water is carbon neutral and sunlight is a sustainable energy source.

A key challenge for water splitting is developing catalysts for
35 the direct and efficient production of hydrogen from protons. Platinum and other heterogeneous precious metal catalysts have been studied for hydrogen generation for decades, but ultimately suffer from high cost and low abundance.⁷⁻⁹ Alternatively, solid-state catalysts composed of earth-abundant elements, such as
40 metal alloys and molybdenum sulfides, have also been investigated.^{5,10-19} However, it remains a challenge to rationally assess precise structure-activity relationships in these heterogeneous systems. Enzymes like hydrogenases that utilize earth-abundant metals offer an attractive approach to hydrogen
45 evolution catalysis with high catalytic activity and efficiency; however, it is difficult to integrate hydrogenases into solar water-splitting devices owing to their large size and relative long-term instability. Enzyme mimics provide exquisite insight into biological systems and lay the groundwork for new catalyst
50 design principles, but they often function in organic solvents with organic acids.²⁰⁻²³ As such, a growing number of abiotic molecular catalysts for electrocatalytic and photocatalytic hydrogen production featuring earth-abundant elements,²⁴ including iron,²⁵⁻²⁷ cobalt,²⁸⁻³⁷ nickel,³⁸⁻⁴² and molybdenum,⁴³⁻⁴⁵

55 are being reported.

An important step forward for the field of H₂ catalysis is the development of systems that can operate in aqueous media, because using water as both the substrate and solvent increases substrate concentration while minimizing organic additives and
60 waste by-products. As a molecular approach toward this end, we recently reported that a cobalt pentapyridine complex, [(PY5Me₂)Co(H₂O)](CF₃SO₃)₂ (**2**; PY5Me₂ = 2,6-bis(1,1-

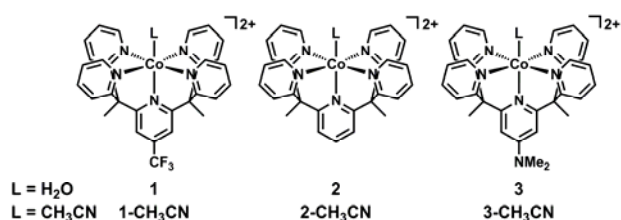


Fig. 1 Molecular cobalt pentapyridine complexes for catalytic H₂
65 generation.

di(pyridin-2-yl)ethyl)pyridine; see Fig. 1) is a robust and efficient electrocatalyst for hydrogen evolution in pH 7 buffer on a mercury electrode, albeit at fairly high overpotential.⁴⁶ However, the tunability of the PY5Me₂ platform allowed us to modify the
70 para-position of its central pyridine and synthesize the derivative [(CF₃PY5Me₂)Co(H₂O)](CF₃SO₃)₂ (**1**), which showed a positive shift in both the Co(II)/Co(I) reduction potential and the overpotential for H₂ catalysis. To demonstrate that the performance of this catalyst is not restricted to electrochemistry
75 on mercury, which can adsorb molecular species,²⁸ we now report that **1** is indeed a versatile system for electro- and photochemical H₂ generation in water. In particular, we show that it is a competent electrocatalyst under soluble, diffusion-limited conditions using a glassy carbon electrode, and, importantly, that

it can function as a photocatalyst in combination with either a simple molecular chromophore such as $[\text{Ru}(\text{bpy})_3]^{2+}$ or a semiconductor GaP nanowire photosensitizer system.⁴⁷

Results and Discussion

5 Catalytic hydrogen generation on a glassy carbon electrode

Since the exogenous ligand L at the apical position of the PY5-cobalt complexes is exchangeable and sensitive to solvent, we chose to synthesize **1-CH₃CN** for electrochemical studies in acetonitrile, while using the aquo complex **1** for experiments conducted in aqueous media. Employing these complexes avoids possible solvent contamination in electrochemical studies. Similar to our previous report, metalation of $\text{CF}_3\text{PY5Me}_2$ with $\text{Co}(\text{CF}_3\text{SO}_3)_2(\text{MeCN})_2$ in acetonitrile at room temperature results in the formation of **1-CH₃CN**, the crystal structure of which is shown in Fig. S1.⁴⁶ In agreement with the reported structure of **2-CH₃CN**, the Co(II) center in **1-CH₃CN** resides in a slightly distorted octahedral geometry with acetonitrile bound at the apical site. The structure of **1** has been reported previously.⁴⁶

The cyclic voltammogram of **1-CH₃CN** in acetonitrile solution features two reversible redox processes at $E_{1/2} = 0.98$ V and -0.64 V vs SHE, assigned to metal-based Co(III)/Co(II) and Co(II)/Co(I) couples, respectively, with another irreversible reduction peak at -1.57 V vs SHE (Fig. S2). Compared to the redox processes observed for parent PY5Me₂ complex **2-CH₃CN** in acetonitrile, CF₃ substitution on the *para* position of the central pyridine ring positively shifts the formal Co(III)/(II), Co(II)/(I), and Co(I)/(0) couples of **1-CH₃CN** by ca. 105, 140 and 120 mV, respectively. As the free ligand CF₃PY5Me₂ is redox-silent in the same potential region (see Fig. S3), the data suggest that these observed features are metal-dependent.

Owing to the large overpotential of **2** for hydrogen evolution catalysis and the relative small electrochemical window of the glassy carbon electrode in pH 7 aqueous media, no apparent

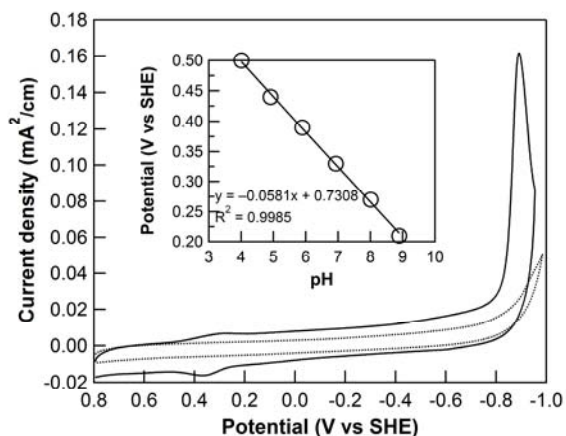


Fig. 2 Cyclic voltammograms of 0.1 mM **1** (solid line) and blank glassy carbon electrode (dotted line) in 0.1 M phosphate buffer at pH 7. Inset: pH dependence of the oxidation peak of **1** in 0.1 M buffered electrolytes at various pH values. Conditions: 0.1 M NaClO₄ added as the supporting electrolyte, scan rate = 100 mV/s, Ar atmosphere.

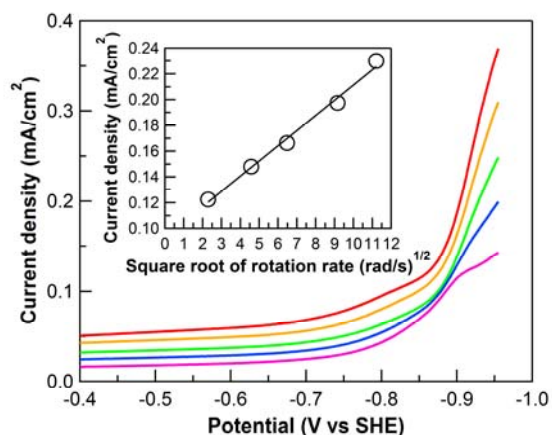


Fig. 3 Cathodic scans of 0.3 mM **1** in 0.1 M phosphate buffer and 0.1 M NaClO₄ at pH 7 at different rotating rates: 100 (purple), 400 (blue), 800 (green), 1600 (orange), 2400 (red) rpm, (scan rate: 25 mV/s). Inset: Levich plot of current density at overpotential = 500 mV versus the square root of rotating rate.

reduction feature of **2** was observed before the rise of the glassy carbon background current. In contrast, the CF₃ derivative **1** exhibits a well-resolved and irreversible cathodic peak at -0.89 V vs SHE in 0.1 M phosphate buffered to pH 7, with a much more pronounced rise in current density compared to the background (Fig. 2). In the positive potential direction, a reversible redox feature at 0.35 V vs SHE was also observed. The pH-dependent cyclic voltammograms of **1** in 0.1 M phosphate buffer with 0.1 M NaClO₄ as the supporting electrolyte are shown in Fig. S4. The oxidation wave shifts positively along the decrease of pH from 9 to 4, with a slope of 58.1 mV/pH (inset of Fig. 2), indicating a one-proton and one-electron redox process close to the ideal value of 59 mV/pH. This observation led us to assign the oxidation wave as a Co(II)-OH₂/Co(III)-OH couple. Similar results have been reported for other cobalt complexes with pentadentate ligands in aqueous medium.^{35,48} The pH-dependence of the reduction feature is more complex and is a topic under current investigation.

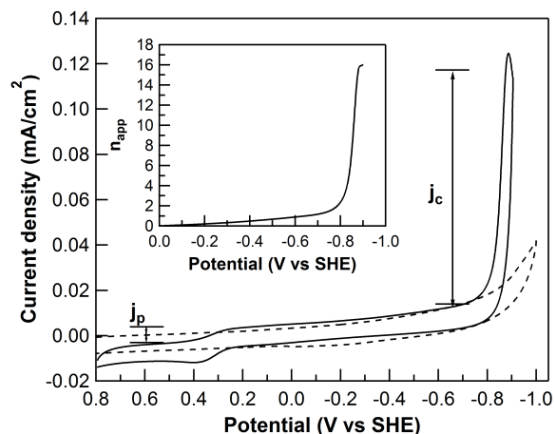


Fig. 4 Rotating disk electrode voltammograms of 0.1 mM **1** (solid) and blank glassy carbon electrode (dotted) in 0.1 M phosphate buffer at pH 7. Inset: n_{app} plot of **1** versus potential. Conditions: 0.1 M NaClO₄ added as the supporting electrolyte, scan rate = 25 mV/s, rotation rate = 400 rpm/s, Ar atmosphere.

Rotating disk electrode voltammetry (RDEV) studies

To demonstrate the molecular nature of cobalt pentapyridine complex as a hydrogen generation catalyst in aqueous media, a rotating disk electrode (RDE) was utilized to probe the hydrodynamics of the system in 0.1 M phosphate buffer at pH 7. Fig. 3 displays the RDE voltammograms of **1** at different rotation rates with a scan rate of 25 mV/s. A linear Levich plot of the current density at 0.900 V vs SHE versus the square root of the rotation rate was obtained (inset of Fig. 3), indicating that the catalytic current is under diffusion control.

In order to compare the performance of **1** to that of other hydrogen catalysts in aqueous media, we sought to determine its apparent rate of proton reduction utilizing a method recently reported by Peters and co-workers.³³ The parameter n_{app} , defined as the apparent number of electrons delivered to the catalyst before it diffuses away from the electrode surface, can be calculated by the electrocatalytic current density normalized for the delivery of the catalyst to the surface as illustrated in eq 1.

$$n_{\text{app}} = \frac{j_c}{j_p} \quad (1)$$

Here, j_p is the plateau current density for the Co(II)-aqua/Co(III)-hydroxide couple and j_c is the catalytic current density as shown in its RDE voltammogram (Fig. 3). The plot of n_{app} versus potential for **1** is included in the inset of Fig 3. The value of n_{app} increases dramatically after the onset of catalysis at ca. -0.8 V vs SHE, consistent with the cyclic voltammogram in Fig. 2, reaching nearly 16 at -0.900 V vs SHE (overpotential = -487 mV). Compared to the reported n_{app} values of 1-8 for a series of cobalt complexes at an overpotential of ca. -500 mV in pH 2.2 buffers,³³ which were measured at the same scan rate and rotation rate as this present study, **1** exhibits better efficiency as a hydrogen evolution catalyst in neutral pH aqueous solution at approximately the same overpotential. Similar results were obtained in the 0.2 M NaClO₄ (Figs S5 and S6), indicating that phosphate does not play a special role in this system. In addition, a Faradaic efficiency of 95 ± 10 % was measured by gas

chromatography for a 3-h bulk electrolysis of **1** at an applied potential of -0.963 V vs SHE (overpotential = -550 mV) in pH 7 buffer (Fig. 5). The used glassy carbon plate was rinsed with water and used as the working electrode in fresh buffer for another blank bulk electrolysis, which passed much less charge under the same condition (Fig. 5). These results demonstrate the efficacy of **1** as an efficient and robust molecular electrocatalyst for hydrogen evolution reaction.

Photocatalytic hydrogen production using a molecular photosensitizer

After establishing that the cobalt pentapyridine complex **1** is a competent molecular electrocatalyst for hydrogen evolution in neutral water under diffusion-limited conditions, we next tested whether it could also be utilized as a photocatalyst under similar conditions. To this end, we carried out photocatalysis experiments in neutral aqueous solutions using [Ru(bpy)₃]Cl₂ as a soluble molecular inorganic photosensitizer and ascorbic acid as an electron donor. As shown in Fig. 6a and Fig. S7, upon irradiation with light of wavelength $\lambda_{\text{irr}} \geq 455$ nm at room temperature, a solution of 50 μ M catalyst, 0.2 mM [Ru(bpy)₃]Cl₂, and 0.1 M ascorbic acid in 1.0 M phosphate buffer at pH 7 evolves hydrogen. The hydrogen evolution rate is initially linear in the first 2 h, followed by a slight deviation, until reaching the plateau of ca. 0.5 mL after 8 h of photolysis. In a separate experiment, we tested the stability of catalyst **1** and the chromophore during photolysis. As shown in Fig S8, after 10 h photolysis, further addition of 0.2 mM chromophore resumes nearly 40% activity of **1** under another 4 h illumination, indicating that although some of the catalyst may deactivate during the first 10-h photolysis, chromophore decomposition is the primary reason for the cease of hydrogen evolution after 8-h illumination.³⁵ Importantly, control experiments without photosensitizer or ascorbic acid showed no H₂ generation, and in the absence of catalyst, only negligible hydrogen was detected under the same conditions (Fig. 6a and Fig. S7), establishing that all three components are necessary for the efficient photocatalytic evolution of hydrogen from water.³⁵ Compared to the photocatalytic hydrogen evolution catalyzed by **2** and **3** (Fig. 6a),

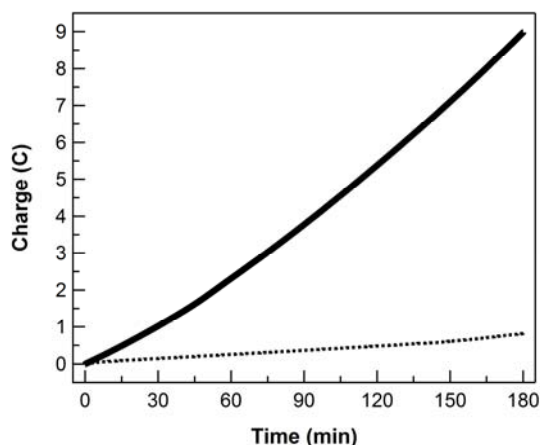


Fig. 5 Controlled potential electrolysis of 0.1 mM **1** (solid) and rinsed glassy plate after bulk electrolysis of **1** (dotted) in 0.1 M phosphate buffer and 0.1 M NaClO₄ at pH 7, showing charge build-up versus time with an applied potential of -0.963 V vs SHE (overpotential = -550 mV).

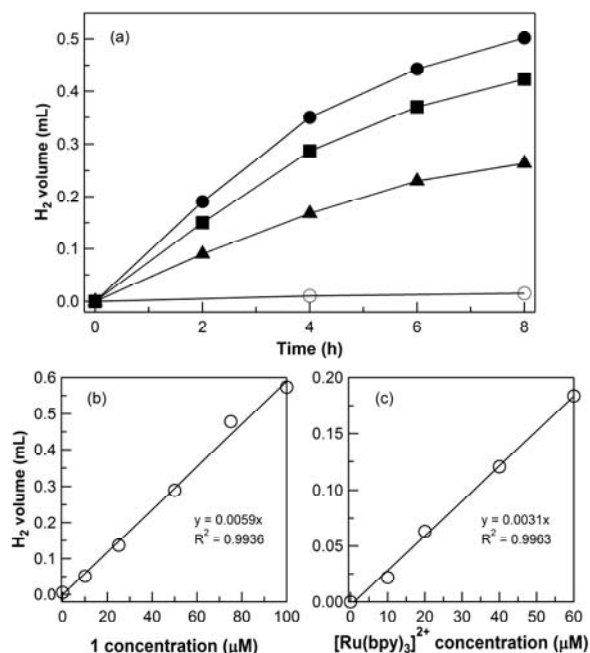


Fig. 6 (a) Photocatalytic hydrogen evolution over time as measured by gas chromatography for aqueous solutions containing 50 μM **1** (filled circles), 50 μM **2** (filled squares), 50 μM **3** (filled triangles), or no catalyst (open circles) with 0.2 mM $[\text{Ru}(\text{bpy})_3]\text{Cl}_2$ and 0.1 M ascorbic acid in 1.0 M phosphate buffer of pH 7. (b) Photogenerated hydrogen volume after 2 h of illumination ($\lambda_{\text{irr}} \geq 455$ nm) of 0.2 mM $[\text{Ru}(\text{bpy})_3]\text{Cl}_2$ and 0.1 M ascorbic acid in 1.0 M phosphate buffer of pH 7 with various concentrations of **1**. (c) Photogenerated hydrogen volume after 2 hour illumination ($\lambda_{\text{irr}} \geq 455$ nm) of 50 μM **1** and 0.1 M ascorbic acid in 1.0 M phosphate buffer of pH 7 with various concentrations of $[\text{Ru}(\text{bpy})_3]\text{Cl}_2$. The light source was a 150 W Xe lamp coupled to a 455-nm long-pass filter.

it is clear that **1** exhibits the highest catalytic performance under the conditions measured, which is consistent with its lower overpotential for electrocatalysis of hydrogen evolution in neutral water.⁴⁶ During the first two hours of photolysis, an average quantum yield of 0.23% was obtained for 50 μM **1** in the presence of 0.2 mM $[\text{Ru}(\text{bpy})_3]^{2+}$ and 0.1 M ascorbic acid. With increasing concentrations of catalyst, the average quantum yield during the first two hours of photolysis reached a plateau of ~0.6 % under the same conditions (Fig. S9).

To explore the effects of catalyst concentration on photochemical hydrogen generation, a series of 2-h photolysis experiments were carried out with various concentrations of **1**. It is clear from Fig. 6b that, within the concentration range less than 100 μM , the H_2 evolution rate is first-order in catalyst concentration. An analogous observation has been made for other cobalt diglyoxime catalysts and a recent cobalt-ditholene catalyst, albeit in different solutions.^{36,49} Similarly, the effect of chromophore concentration on the system activity was also investigated. As shown in Fig. 6c, with the catalyst concentration kept constant at 50 μM and at relatively low concentrations of the photosensitizer (< 60 μM), a linear relationship between hydrogen evolution rate and chromophore concentration was obtained. We note that at higher photosensitizer concentrations, the system activity is limited by the intrinsic efficiency of the catalyst.

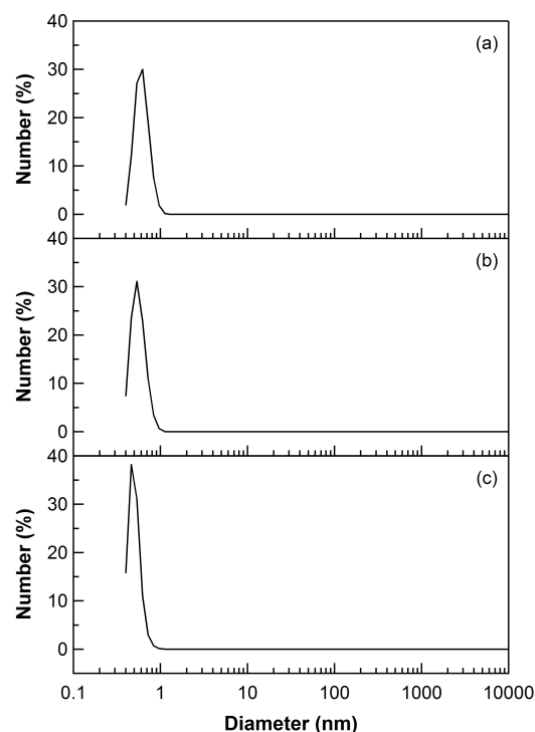


Fig. 7 Particle size distribution of photolysis solutions containing 50 μM **1**, 0.2 mM $[\text{Ru}(\text{bpy})_3]\text{Cl}_2$, and 0.1 M ascorbic acid in 1.0 M phosphate buffer of pH 7 after illumination ($\lambda_{\text{irr}} \geq 455$ nm) of 0 h (a), 0.5 h (b), and 3 h (c), determined by dynamic light scattering measurements.

Sav ant and co-workers recently reported that in the presence of strong acids, the boron-capped tris(glyoximate) cobalt clathrochelate complexes decompose to form cobalt-containing nanoparticles that are actually responsible for the observed H_2 generation activity.^{50,51} In addition, considering the concerns on the homogeneous or heterogeneous nature of some water oxidation cobalt catalysts published recently,^{52–54} we decided to investigate whether H_2 evolution detected during photolysis may come from colloidal nanoparticle or other heterogeneous cobalt species. To this end, dynamic light scattering (DLS) measurements were conducted for photolysis solutions after 0 h, 0.5 h, and 3 h of irradiation ($\lambda_{\text{irr}} \geq 455$ nm) at room temperature. As shown in Fig. 7, no species with a diameter larger than 1 nm could be detected in any of the three samples. Although we cannot unambiguously rule out any small particulate species, the different photocatalytic performance of the three cobalt catalysts with similar ligand platform, the first-order dependence on catalyst and photosensitizer, along with no evidence for particle formation at > 1 nm sizes under the current photolysis conditions, strongly suggest the involvement of a molecular species.

65 Photocatalytic hydrogen production using a semiconductor nanowire photosensitizer

Owing to the scarcity and hence high cost of ruthenium-based photosensitizers, it is desirable to replace $[\text{Ru}(\text{bpy})_3]^{2+}$ with other chromophores composed of earth-abundant elements. As such, semiconductors possessing a high conduction band edge and visible light absorption offer a promising light-harvesting alternative.⁹ We recently reported the surfactant-free synthesis and characterization of GaP nanowires exhibiting hydrogen

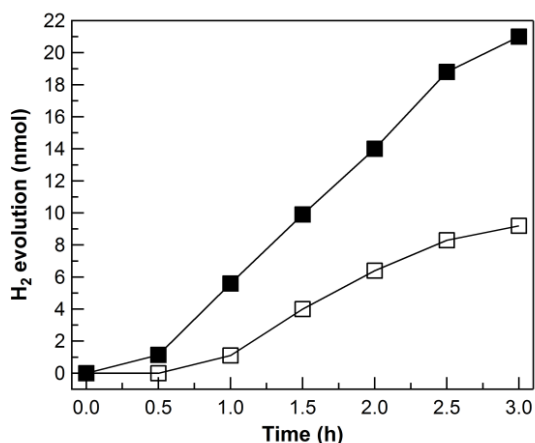


Fig. 8 Photocatalytic hydrogen evolution over time using a 0 mM (white square) and 0.2 mM (black square) solutions of **1** in the presence of 1 mg of GaP nanowires in 2.5 mL H₂O with 0.5 mL of methanol added as the electron donor. The light source was a 450-W Xe lamp coupled to a 400-nm long-pass filter.

generation activity under visible light irradiation in water.⁴⁷ To test whether our molecular cobalt catalyst could enhance H₂ evolution performance, a photolysis experiment was conducted with 0.2 mM **1** and 1 mg of GaP nanowires in water, using methanol as a hole scavenger. The diameter and length of the nanowires were ~40 nm and > 1 μm, respectively. Indeed, as shown in Fig. 8, the hydrogen evolution rate is patently increased in the presence of catalyst **1**, with a five-fold enhancement compared to the control sample during the first hour. Because hydrogen is quantified by head space gas sampling, we note that the hydrogen observed during the first 30 min is potentially low as a result of it being mainly dissolved in the electrolyte. Likewise, the decreased rate of hydrogen evolution after 2.5 h of photolysis may be due to the aggregation of GaP nanowires and/or decomposition of the catalysts. In addition, we observe that higher catalyst concentrations generally result in nanowire aggregation, which precludes quantitative analysis at this time. Since **1** is a relatively bulky molecular catalyst and the biomolecular electron-transfer rate between the GaP nanowires and cobalt complex **1** highly depends on their efficient collision, which is strikingly different from our reported Pt-coated GaP system,⁴⁷ we believe that the hydrogen evolution performance can be improved upon by tuning electron transfer via covalent catalyst attachment or other means.

Conclusions

In summary, we have shown that the cobalt pentapyridine complex $[(CF_3PY_5Me_2)Co(H_2O)]^{2+}$ is a competent molecular catalyst for the electrochemical production of hydrogen from neutral pH water under soluble, diffusion-limited conditions. Furthermore, the complex **1** can be employed as a photocatalyst for hydrogen evolution in neutral water, using $[Ru(bpy)_3]^{2+}$ as a molecular photosensitizer and ascorbic acid as the sacrificial electron donor. Dynamic light scattering measurements show no evidence for nanoparticle formation for the duration of the photolysis reactions, and photocatalysis is first-order in both catalyst and photosensitizer. We further demonstrated that **1** can operate in conjunction with a semiconductor photosensitizer, GaP

nanowires, to enhance the hydrogen yield of photolysis upon visible light irradiation in water. These results present a starting point for constructing a molecular catalyst/semiconductor photosensitizer assembly using all earth-abundant components for H₂ evolution catalysis in pure aqueous solution. Current lines of investigation include: performing further ligand modifications to decrease the overpotential and increase the rate of catalysis, strengthening the association between the molecular catalysts and the GaP nanowires to enhance the electron transfer, and coupling this reductive solar-driven process to oxidative oxygen evolution to generate a complete solar-to-fuel water-splitting system.

Experimental Section

Materials

$Ru(bpy)_3Cl_2$, 4-trifluoromethyl-2,6-bis[(2-pyridyl)ethyl]pyridine ($CF_3PY_5Me_2$), $[(CF_3PY_5Me_2)Co(H_2O)](CF_3SO_3)_2$ (**1**), and GaP nanowires were synthesized and purified as previously reported.^{46,55,56} Glassy carbon rods (type 1) were purchased from Alfa Aesar for the electrochemical studies. Acetonitrile was dried over activated 4 Å molecular sieves, passed through a column of activated alumina, and stored over 3 Å molecular sieves under a nitrogen atmosphere. Water was deionized with the Millipore Milli-Q UF Plus system. All other chemical reagents were purchased from commercial vendors and used without further purification. Unless noted otherwise, all manipulations were carried out at room temperature under a nitrogen atmosphere in a VAC glovebox or using high-vacuum Schlenk line techniques.

Syntheses

$[(CF_3PY_5Me_2)Co(NCCH_3)](CF_3SO_3)_2$ (**1-CH₃CN**) 1 eq of $Co(CF_3SO_3)_2(CH_3CN)_2$ (175 mg) was added to a 5 mL acetonitrile suspension of $CF_3PY_5Me_2$ (177 mg). The mixture was stirred under nitrogen atmosphere at room temperature for 5 h. The orange solution was then concentrated to ~ 1 mL under vacuum and diethyl ether vapor diffusion into this solution generated rod-shape light brown crystals suitable for X-ray crystallography. Yield: 312 mg (93%). LC-MS (M^+) m/z calcd for $C_{30}H_{25}CoF_3N_5O_3S$ 651.0962, found 651.0947.

Physical Methods

Carbon, hydrogen, and nitrogen analyses were obtained from the Microanalytical Laboratory of the University of California, Berkeley. Cyclic voltammetry experiments were carried out using BASI's Epsilon potentiostat and C-3 cell stand. A glassy carbon working electrode, a silver wire reference electrode, a platinum wire counter electrode were used for cyclic voltammetry experiments in CH_3CN with 0.1 M Bu_4NPF_6 in glovebox. Ferrocene (E^0 of $Fc^+/Fc = 0.64$ V vs SHE) was added during each experiment as an internal reference. For electrochemical studies conducted in aqueous media, a glassy carbon (3 mm diameter) was used as the working electrode and platinum wire as the auxiliary electrode. The reference electrode was a commercially available aqueous Ag/AgCl electrode, and the potentials were reported with respect to SHE by adding 0.195 V to the experimentally measured values. The electrolyte solution was thoroughly deaerated via bubbling argon 30 min prior to each electrochemical measurement in water and kept under positive argon pressure during the experiments. An Agilent 490-GC Micro-Gas Chromatograph with a molecular sieve column and

heated syringe injector was used for hydrogen detection and quantification. The column was heated to 80 °C under Ar gas flow and an average sample volume of 200 nL was injected onto the column for each measurement. The ratio of the integrated areas of the hydrogen peak versus the internal standard methane peak was compared to a calibration curve (Fig. S10) to calculate the hydrogen volume generated. A 150 W USHIO Xenon lamp with a 3 mm 455 nm optical glass filter was used to irradiate the photolysis sample solution which is kept in a water bath with cooling water circulating during the entire experiment.

Crystallographic Structure Determinations

The X-ray crystallographic data collection was carried out on a Bruker three-circle diffractometer mounted with an SMART 1000 detector using monochromated Mo K α radiation (0.71073 Å) outfitted with a low-temperature, nitrogen-stream aperture, an APEXII CCD detector, and equipped with an Oxford Cryostream 700. The structure was solved using direct methods in conjunction with standard difference Fourier techniques and refined by full-matrix least-squares procedures.¹ A semi-empirical absorption correction (SADABS) was applied to the diffraction data for all structures. All non-hydrogen atoms were refined anisotropically, and hydrogen atoms were treated as idealized contributions and refined isotropically. A summary of crystallographic data is given in Table S1. All software used for diffraction data processing and crystal-structure solution and refinement are contained in the APEX2 program suite (Bruker AXS, Madison, WI).

Photolysis experiments

Samples of 4 mL solutions were prepared with known concentrations of catalyst, [Ru(bpy)₃]Cl₂, and ascorbic acid in 1.0 M phosphate buffer at pH 7 in a 30 mL schlenk flask sealed by a rubber septum with copper wire. The sample solutions were thoroughly deaerated by argon bubbling for 30 min prior to photolysis experiment. Each sample was irradiated by a USHIO 150 W Xenon lamp ($\lambda \geq 455$ nm) or a 450 W Xenon lamp ($\lambda \geq 400$ nm) at room temperature under constant stirring. The amounts of hydrogen produced during photolysis were determined by gas chromatography using methane as an internal standard. Quantum yields were determined following the procedure outlined in *Handbook of Photochemistry*, using ferrioxalate as the standard.⁵⁷

Acknowledgements

The synthetic and catalytic portions of this work were supported by DOE/LBNL Grant 403801 (C.J.C.). The contributions of J.R.L. were supported by NSF grant CHE-1111900. The nanowire part of this study was supported by the Director, Office of Science, Office of Basic Energy Sciences, Materials Sciences and Engineering Division, of the U.S. Department of Energy under Contract No. DE-AC02-05CH11231 (P.Y.). C.J.C. is an Investigator with the Howard Hughes Medical Institute.

Notes and references

^aDepartment of Chemistry and the ^bHoward Hughes Medical Institute, University of California, Berkeley, California 94720, United States; ^cChemical Sciences Division, ^dJoint Center for Artificial Photosynthesis (JCAP), ^eMaterials Sciences Division,, Lawrence Berkeley National

Laboratory, Berkeley, California 94720, United States; Email: chrischang@berkeley.edu; p_yang@berkeley.edu; jrlong@berkeley.edu.

†Electronic Supplementary Information (ESI) available: X-ray crystallography data and structure of 2-CH₃CN (CCDC 894807), electrochemistry data in CH₃CN and NaClO₄, additional photolysis data, gas chromatograms, and hydrogen calibration curves. See DOI: 10.1039/b000000x/

- 1 A. J. Bard and M. A. Fox, *Acc. Chem. Res.*, 1995, **28**, 141-145.
- 2 J. A. Turner, *Science*, 2004, **305**, 972-974.
- 3 N. S. Lewis and D. G. Nocera, *Proc. Natl. Acad. Sci.*, 2006, **103**, 15729-15735.
- 4 D. G. Nocera, *Chem. Soc. Rev.*, 2009, **38**, 13-15.
- 5 T. R. Cook, D. K. Dogutan, S. Y. Reece, Y. Surendranath, T. S. Teets and D. G. Nocera, *Chem. Rev.*, 2010, **110**, 6474-6502.
- 6 M. G. Walter, E. L. Warren, J. R. McKone, S. W. Boettcher, Q. Mi, E. A. Santori and N. S. Lewis, *Chem. Rev.*, 2010, **110**, 6446-6473.
- 7 A. Fujishima and K. Honda, *Nature*, 1972, **238**, 37-38.
- 8 E. Aharon-Shalom and A. Heller, *J. of Electrochem. Soc.*, 1982, **129**, 2865-2866.
- 9 X. Chen, S. Shen, L. Guo and S. S. Mao, *Chem. Rev.*, 2010, **110**, 6503-6570.
- 10 S. Trasatti, *J. Electroanal. Chem.*, 1972, **39**, 163-184.
- 11 B. E. Conway, L. Bai and M. A. Sattar, *Int. J. Hydrogen Energy*, 1987, **12**, 607-621.
- 12 O. Savadogo and H. Lavoie, *Int. J. Hydrogen Energy*, 1992, **17**, 473-477.
- 13 O. Savadogo, *J. Electrochem. Soc.*, 1992, **139**, 1082-1087.
- 14 O. Savadogo, F. Carrier and E. Forget, *Int. J. Hydrogen Energy*, 1994, **19**, 429-435.
- 15 B. Hinnemann, P. G. Moses, J. Bonde, K. P. Jorgensen, J. H. Nielsen, S. Horch, I. Chorkendorff and J. K. Nørskov, *J. Am. Chem. Soc.*, 2005, **127**, 5308-5309.
- 16 T. F. Jaramillo, K. P. Jorgensen, J. Bonde, J. H. Nielsen, S. Horch and I. Chorkendorff, *Science*, 2007, **317**, 100-102.
- 17 Y. Li, H. Wang, L. Xie, Y. Liang, G. Hong and H. Dai, *J. Am. Chem. Soc.*, 2011, **133**, 7296-7299.
- 18 D. Merki, S. Fierro, H. Vrubel and X. Hu, *Chem. Sci.*, 2011, **2**, 1262-1267.
- 19 D. Merki, H. Vrubel, L. Rovelli, S. Fierro and X. Hu, *Chem. Sci.*, 2012, **3**, 2515-2525.
- 20 V. Artero and M. Fontecave, *Coord. Chem. Rev.*, 2005, **249**, 1518-1535.
- 21 P. D. Tran, V. Artero and M. Fontecave, *Energy Environ. Sci.*, 2010, **3**, 727-747.
- 22 A. M. Appel, D. L. DuBois and M. R. DuBois, *J. Am. Chem. Soc.*, 2005, **127**, 12717-12726.
- 23 B. E. Barton, C. M. Whaley, T. B. Rauchfuss and D. L. Gray, *J. Am. Chem. Soc.*, 2009, **131**, 6942-6943.
- 24 P. Du and R. Eisenberg, *Energy Environ. Sci.*, 2012, **5**, 6012-6021.
- 25 I. Bhugun, D. Lexa and J.-M. Saveant, *J. Am. Chem. Soc.*, 1996, **118**, 3982-3983.
- 26 J. W. Tye, J. Lee, H.-W. Wang, R. Mejia-Rodriguez, J. H. Reibenspies, M. B. Hall and M. Y. Darensbourg, *Inorg. Chem.*, 2005, **44**, 5550-5552.
- 27 M. J. Rose, H. B. Gray and J. R. Winkler, *J. Am. Chem. Soc.*, 2012, **134**, 8310-8313.
- 28 P. V. Bernhardt and L. A. Jones, *Inorg. Chem.*, 1999, **38**, 5086-5090.
- 29 J. P. Bigi, T. E. Hanna, W. H. Harman, A. Chang and C. J. Chang, *Chem. Commun.*, 2010, **46**, 958-960.
- 30 V. Fourmond, P.-A. Jacques, M. Fontecave and V. Artero, *Inorg. Chem.*, 2010, **49**, 10338-10347.
- 31 X. Hu, B. M. Cossairt, B. S. Brunschwig, N. S. Lewis and J. C. Peters, *Chem. Commun.*, 2005, 4723-4725.
- 32 X. Hu, B. S. Brunschwig and J. C. Peters, *J. Am. Chem. Soc.*, 2007, **129**, 8988-8998.
- 33 C. C. L. McCrory, C. Uyeda and J. C. Peters, *J. Am. Chem. Soc.*, 2012, **134**, 3164-3170.

-
- 34 B. D. Stubbert, J. C. Peters and H. B. Gray, *J. Am. Chem. Soc.*, 2012, **133**, 18070-18073.
- 35 W. M. Singh, T. Baine, S. Kudo, S. Tian, X. A. N. Ma, H. Zhou, N. J. DeYonker, T. C. Pham, J. C. Bollinger, D. L. Baker, B. Yan, C. E. Webster and X. Zhao, *Angew. Chem., Int. Ed.*, 2012, **51**, 5941–5944.
- 36 W. R. McNamara, Z. Han, P. J. Alperin, W. W. Brennessel, P. L. Holland and R. Eisenberg, *J. Am. Chem. Soc.*, 2012, **133**, 15368-15371.
- 37 W. R. McNamara, Z. Han, C.-J. M. Yin, W. W. Brennessel, P. L. Holland and R. Eisenberg, *Proc. Natl. Acad. Sci.*, doi:10.1073/pnas.1120757109.
- 38 A. Le Goff, V. Artero, B. Jusselme, P. D. Tran, N. Guillet, R. Métayé, A. Fihri, S. Palacin and M. Fontecave, *Science*, 2009, **326**, 1384-1387.
- 39 A. D. Wilson, R. H. Newell, M. J. McNevin, J. T. Muckerman, R. M. DuBois and D. L. DuBois, *J. Am. Chem. Soc.*, 2006, **128**, 358-366.
- 40 U. J. Kilgore, J. A. S. Roberts, D. H. Pool, A. M. Appel, M. P. Stewart, M. R. DuBois, W. G. Dougherty, W. S. Kassel, R. M. Bullock and D. L. DuBois, *J. Am. Chem. Soc.*, 2012, **133**, 5861-5872.
- 41 M. L. Helm, M. P. Stewart, R. M. Bullock, M. R. DuBois and D. L. DuBois, *Science*, 2011, **333**, 863-866.
- 42 D. H. Pool, M. P. Stewart, M. O'Hagan, W. J. Shaw, J. A. S. Roberts, R. M. Bullock and D. L. DuBois, *Proc. Natl. Acad. Sci.*, 2012, DOI: 10.1073/pnas.1120208109.
- 43 H. I. Karunadasa, C. J. Chang and J. R. Long, *Nature*, 2010, **464**, 1329-1333.
- 44 H. I. Karunadasa, E. Montalvo, Y. Sun, M. Majda, J. R. Long and C. J. Chang, *Science*, 2012, **335**, 698-702.
- 45 V. S. Thoi, H. I. Karunadasa, Y. Surendranath, J. R. Long and C. J. Chang, *Energy Environ. Sci.*, 2012, **5**, 7762-7770.
- 46 Y. Sun, J. P. Bigi, N. A. Piro, M. L. Tang, J. R. Long and C. J. Chang, *J. Am. Chem. Soc.*, 2011, **133**, 9212-9215.
- 47 J. Sun, C. Liu and P. Yang, *J. Am. Chem. Soc.*, 2011, **133**, 19306-19309.
- 48 D. J. Wasylenko, C. Ganesamoorthy, J. Borau-Garcia and C. P. Berlinguette, *Chem. Commun.*, 2011, **47**, 4249-4251.
- 49 P. Du, J. Schneider, G. Luo, W. W. Brennessel and R. Eisenberg, *Inorg. Chem.*, 2009, **48**, 4952-4962.
- 50 E. Anxolabéhère-Mallart, C. Costentin, M. Fournier, S. Nowak, M. Robert and J.-M. Savéant, *J. Am. Chem. Soc.*, 2012, **134**, 6104-6107.
- 51 Y. Z. Voloshin, A. V. Dolganov, O. A. Varzatskii and Y. N. Bubnov, *Chem. Commun.*, 2011, **47**, 7737-7739.
- 52 Q. Yin, J. M. Tan, C. Besson, Y. V. Geletii, D. G. Musaev, A. E. Kuznetsov, Z. Luo, K. I. Hardcastle and C. L. Hill, *Science*, 2010, **328**, 342-345.
- 53 J. J. Stracke and R. G. Finke, *J. Am. Chem. Soc.*, 2011, **133**, 14872-14875.
- 54 D. J. Wasylenko, R. D. Palmer, E. Schott and C. P. Berlinguette, *Chem. Commun.*, 2012, **48**, 2107-2109.
- 55 Y. Sun, D. A. Lutterman and C. Turro, *Inorg. Chem.*, 2008, **47**, 6427-6434.
- 56 J. Sun, C. Liu and P. Yang, *J. Am. Chem. Soc.*, 2011, **133**, 19306-19309.
- 57 S. L. Murov, I. Carmichael and G. L. Hug, *Handbook of Photochemistry*, Marcel Dekker, New York, 1993.

Acknowledgements: This work was supported by the Director, Office of Science, Office of Basic Energy Sciences, Material Sciences and Engineering Division, of the U.S. Department of Energy under Contract No. DE-AC02-05CH11231. We thank the National Center for Electron Microscopy for the use of their facilities.